

1 **Title and authorship information:**

2 **Dual specificity phosphatase 7 drives the formation of cardiac mesoderm**
3 **in mouse embryonic stem cells**

4 **Stanislava Sladeček¹, Katarzyna Anna Radaszkiewicz¹, Martina Bóhmová¹, Tomáš Gybel¹,**
5 **Tomasz Witold Radaszkiewicz¹, Jiří Pacherník^{1*}**

6 *** Correspondence:**

7 Jiří Pacherník

8 jipa@sci.muni.cz

9 **Affiliations:**

10 ¹Department of Experimental Biology, Faculty of Science, Masaryk University, Brno, Czech Republic

11 **Keywords: DUSP7, MAKP, cardiomyogenesis, mouse embryonic stem cells, mesoderm.**

12 **Abstract**

13 Dual specificity phosphatase 7 (DUSP7) is a protein belonging to a broad group of phosphatases that
14 can dephosphorylate phosphoserine/phosphothreonine as well as phosphotyrosine residues within the
15 same substrate. DUSP7 has been linked to the negative regulation of mitogen activated protein kinases
16 (MAPK), and in particular to the regulation of extracellular signal-regulated kinases 1 and 2 (ERK1/2).
17 MAPKs play an important role in embryonic development, where their duration, magnitude, and
18 spatiotemporal activity must be strictly controlled by other proteins, among others by DUSPs. In this
19 study, we focused on the effect of DUSP7 depletion on the in vitro differentiation of mouse embryonic
20 stem (ES) cells. We showed that even though DUSP7 knock-out ES cells do retain some of their basic
21 characteristics, when it comes to differentiation, they preferentially differentiate towards neural cells,
22 while the formation of early cardiac mesoderm is repressed. Therefore, our data indicate that DUSP7
23 is necessary for the correct formation of neuroectoderm and cardiac mesoderm during the in vitro
24 differentiation of ES cells.

25 **Introduction**

26 The mitogen activated protein kinase (MAPK) pathway is one of the better described and vigorously
27 studied signaling pathways. MAPK plays an important role in many cellular processes like
28 proliferation, differentiation or apoptosis, and its function has been described in the contexts of animal
29 development, cancer biology, immune response, to name just a few[1]–[3]. The MAPK family includes
30 three kinase subfamilies - extracellular signal-regulated kinases (ERK), c-Jun N-terminal kinases
31 (JNK), and p38 [4]. MAPKs are active when phosphorylated on both threonine and tyrosine residues
32 within their activation loop (TxY motif) and can be inactivated by a number of phosphatases, among
33 which are dual specificity phosphatases (DUSP) [5], [6].

34 The human genome encodes more than twenty members of the DUSP family, although their
35 classification can sometimes differ in literature. DUSPs, similarly to MAPKs, have been studied in
36 many types of cancer lines as well as in embryonic stem cells and animal development. They have
37 been described as important for pluripotency [7]–[9], neural development [10], cardiac development
38 [11], immunity [12], and cancer prognosis [13] etc.

39 Dual specificity phosphatase 7 (DUSP7) is a cytoplasmic phosphatase, which dephosphorylates
40 extracellular signal-regulated kinases 1 and 2 (ERK1/2) [14]. The expression of DUSP7 is upregulated,
41 either due to an increase in its expression or stability in some pathological conditions such as leukemia
42 or breast cancer [15]–[17], where it is associated with poor prognosis. Although DUSP7 was studied
43 in cancer cell lines and even sparked interest as a potential cancer drug target [18], it remains one of
44 the less studied DUSPs.

45 In this study, we focused on the role of DUSP7 in mouse embryonic stem (ES) cells and its effect on
46 cell differentiation in vitro. We observed that the depletion of DUSP7 did not change some of the basic
47 characteristics of mouse embryonic stem cells. However, DUSP7 deficiency did lead to changes in cell
48 differentiation through the formation of embryoid bodies. Specifically, differentiating DUSP7 KO cells
49 expressed lower levels of markers typical for mesoderm and, later on, cardiomyocytes, and higher
50 levels of markers typical for ectoderm and, later on, neural progenitors. Together, these data indicate
51 that DUSP7 plays an important role in early neural and cardiac mesoderm development.

52 **Material and Methods**

53 *Cell culture and differentiation*

54 The mouse ES cell line R1 was adapted to feeder-free culture. R1 ES and all genetically modified cell
55 lines derived from them were cultivated as described previously [19]. Undifferentiated cells were
56 cultivated in DMEM media supplemented with 15% FBS, 100 U/ml penicillin, 0.1 mg/ml
57 streptomycin, and 1x non-essential amino acid (all from Gibco-Invitrogen) and 0.05 mM β -
58 mercaptoethanol (Sigma), supplemented with 1 000 U/ml of leukemia inhibitory factor (LIF,
59 Chemicon). Differentiation of the cells was induced by seeding them onto a non-adhesive surface in
60 bacteriological dishes to form floating embryoid bodies or by seeding them in the form of hanging
61 drops (400 cells per 0.03 ml drop), all in medium without LIF. After five days of the cultivation of
62 embryoid bodies, they were transferred to adherent tissue culture dishes and cultivated in DMEM-F12
63 (1:1) supplemented with insulin, transferrin, selenium (ITS, Gibco-Invitrogene), and antibiotics (as
64 above), referred to as ITS medium. Cells were cultivated for up to 21 days depending on individual
65 experiments and the medium was changed every two days. In the case of experiments with genetically
66 selected cardiomyocytes, on day 14 medium was supplemented with 0.5mg/ml of antibiotic G418. An
67 ES cell line for genetically selected cardiomyocytes was prepared subsequently: R1_MHC-neor/pGK-
68 hygro ES cells (referred to as HG8 cells), carrying the Myh6 promoter regulating the expression of
69 neomycin phosphotransferase, were prepared by the transfection of R1 cells by MHC- neor/pGK-hygro
70 plasmid (kindly provided by Dr. Loren J. Field, Krannert Institute of Cardiology, Indianapolis, US).
71 [20].

72 *Creating KO lines using CRISPR-Cas9*

73 DUSP7-null mouse embryonic cell lines were prepared using the CRISPR-Cas9 system as previously
74 described [21], [22]. Guide RNA was designed using the online CHOPCHOP tool [23]. Plasmid
75 pSpCas9(BB)-2A-Puro (PX459) V2.0 (#62988, Addgene) with puromycin resistance was used as the
76 target plasmid to carry the guide RNA. Plasmids were prepared as described previously [24]. For
77 transfection, 24h after passaging, cells were transfected in a serum-free medium using
78 polyethyleneimine (PEI) in a stoichiometry of 6 μ l of PEI per 1 μ g of DNA for 8h. Then, the medium
79 was changed for medium with puromycin (Invivogen, 10ug/ml). Selection lasted for 24h, after which
80 the medium was changed for fresh medium without puromycin, and when formed, colonies of
81 potentially KO cells were picked. Acquired KO cell lines were tested by PCR using the primers
82 TGTTGTGTGAGTCCTGACCG and AGAGGTAGGGCAGGATCTGG (337bp product) for the

83 amplification of genomic DNA, and Hpy166II restriction enzyme (R0616S, New England BioLabs)
 84 (240bp and 97bp products), then verified by next generation sequencing using the Illumina platform,
 85 as described previously [25].

86 *Cell growth*

87 Cells were seeded at a concentration of 1000 cells/cm² and cultivated in full medium for up to 5 days.
 88 From day 3, cells were stained with crystal violet, as previously described [26]. After the colonies had
 89 dried, 10% acetic acid was added to the wells and incubated with shaking for 30min. The absorbance
 90 of the obtained solution was then measured at 550nm on a Sunrise Tecan spectrophotometer.

91 For proliferation analysis using the WST-8 assay, cells were seeded on a culture-treated flat bottom
 92 96-well plate at concentrations of 1000, 500, 250, 125 and 67 cells/well and cultivated in full medium
 93 for 3 days. Cells were incubated with WST-8/Methoxy-PMS (MedChem Expres HY-D0831 and HY-
 94 D0937, final concentration 0,25mg/ml and 2,5ug/ml respectively) for 5 hours and absorbance was
 95 measured at 650 nm and 450 nm on Multiscan GO (Thermo Scientific).

96 For proliferation analysis using the EdU assay, cells were seeded at a concentration of 5000cells/cm²
 97 and cultivated in full medium for 3 days. Cell proliferation was measured using the Click-iT™ Plus
 98 EdU Alexa Fluor™ 488 Flow Cytometry Assay Kit (Thermo Fisher, C10632). Cells were treated with
 99 10 μM EdU (5-ethynyl-2'-deoxyuridine) for one hour prior to harvesting and processed according to
 100 the kit manufacturer's instructions. The untreated cells of each analyzed line were used as a control.
 101 Cells were analyzed using Cytex® Northern Lights spectrum flow cytometry. 20,000 events were
 102 acquired per each sample the percentage of EdU positive cells was analyzed using SpectroFlo software
 103 (Cytex). Single cells were identified and gated by pulse-code processing of the area and the width of
 104 the signal. Cell debris was excluded by using the forward scatter threshold.

105 *Analysis of gene expression by qRT-PCR*

106 Total RNA was extracted by RNeasy Mini Kit (Qiagen). Complementary DNA was synthesized
 107 according to the manufacturer's instructions for RevertAid Reverse Transcriptase (200 U/μL)
 108 (EP0442, Thermo Fisher). qRT-PCR was performed in a Roche Light-cycler using the protocols for
 109 SyberGreen (Roche) or TaqMan (Roche). The protocol for primers using SyberGreen was as follows:
 110 an initial activation step at 95°C for 5 min, followed by 40 cycles at 95°C for 10 s, an annealing
 111 temperature (Table 1) for 10 s, and a temperature of 72°C for 10 s, followed by melting curve
 112 genotyping and cooling. The protocol for primers using TaqMan was as follows: an initial activation
 113 step at 95 °C for 10 min followed by 45 cycles of 95 °C for 10 s, 60 °C for 30 s, and 72 °C for 1 s with
 114 data acquisition. Primer sequences, annealing temperatures, and the probes used are listed in Table 1.
 115 The gene expression of each sample was expressed in terms of the threshold cycle normalized to the
 116 average of at least two so-called house-keeping genes. These were *Actb* and *Tbp* in the case of the
 117 SybrGreen protocol, and *Rpl13a* and *Hprt* in the case of the TaqMan protocol.

118 **Table 1.** Probes and sequences of primers and temperature used in quantitative RT-PCR.

Gene of interest	Forward primer 5' → 3'	Reverse primer 5' → 3'	UPL probe no	Ta (°C)
<i>Hprt</i>	tcctcctcagaccgctttt	cctggttcacatcgctaatac	#95	60
<i>Rpl13a</i>	catgaggtcgggtggaagta	gcctgtttccgtaacctcaa	#25	60
<i>Nkx2.5</i>	gacgtagcctggtgtctcg	gtgtggaatccgtcgaaagt	#53	60
<i>Myh6</i>	cgcatacaaggagctcacc	cctgcagccgcattaagt	#6	60
<i>Myh7</i>	cgcatacaaggagctcacc	ctgcagccgcagtaggtt	#6	60

<i>Mef2c</i>	acccaatcttctgccact	gatctccgccatcagac	#6	60
<i>Gata4</i>	ggaagacacccaatctcg	catggccccacaattgac	#13	60
<i>T</i>	actggctagcctcggagtg	ttgctcacagaccagagactg	#27	60
<i>Mesp1</i>	acccatcgttctgtacgc	gcatgtcgctgctgaagag	#89	60
<i>Sox1</i>	ccagcctccagagcccact	ggcatcgcctcgtgggttt		61
<i>Actb</i>	gatcaagatcattgctcctct	taaacgcgagctcagtaacag		60
<i>Tbp</i>	accgtgaatcttggtgtaaac	gcagcaaatcgcttgggatta		60
<i>Oct4</i>	agaggatcaccttgggttaca	cgaagcgacagatggtggtc		61
<i>Nanog</i>	aggacaggtttcagaagcaga	ccattgctagtcttaaccactg		60
<i>Zfp42</i>	gcacacagaagaagcagga	cactgatccgcaaacacct		59
<i>Fgf5</i>	aagtagcgcgacgttttcttc	ctggaaactgctatgtccgag		61
<i>Klf4</i>	gactaaccttggcgtgag	gggttagcgagttcgaaagg		60
<i>Dusp7</i>	gccatccgctccatcattccc	cagccgtcgtctcgcagcttc		62
<i>Pax6</i>	cgggaaagactagcagccaa	gtgaaggaggagacaggtgtg		62
<i>Afp</i>	tggttacacgaggaagccc	aatgtcggccattccctcac		60
<i>Gata1</i>	gaagcgaatgattgtcagca	cagcagaggtccaggaaaag		61
<i>Gata2</i>	gggagtgtgtcaactgtggt	gcctgttaacattgtgcagc		61
<i>Mash1</i>	ttctccggtctcgtcctactc	ccagttggtaaagtccagcag		62
<i>Tubb3</i>	tgaggcctcctctcacaagta	gtcgggcctgaataggtgtc		62
<i>Dusp6</i>	acctggaaggtggcttcagt	tccgttgcactattggggtc		62

119

120 *Counting of cardiomyocytes*

121 The relative number of cardiomyocytes in differentiating ES cell cultures was determined. For these
 122 experiments, cells that were initially differentiated in the form of hanging drops were used. After 5
 123 days of differentiation, embryoid bodies were transferred to ITS medium in 24-well plates and
 124 cultivated for a total of 20 days. Before analyses, cells were washed with phosphate buffered saline
 125 (PBS), incubated in a 0.3% solution of Collagenase II (Gibco) in DMEM media without serum for 20
 126 minutes, and then incubated in trypsin (0.25% in PBS-EDTA, Gibco) for 5 minutes. Trypsin was
 127 inactivated by adding DMEM media with FBS, and cells in this medium were transferred to a new 24-
 128 well plate and cultivated for a further 24h. Cells were then washed with PBS, fixed for 20min with 4%
 129 formaldehyde, permeabilized by 0.1% TWEEN 20 solution in PBS, and stained using anti-
 130 cardiomyocyte heavy myosin antibody (anti-MHC, clone MF20, kindly provided by Dr. Donald
 131 Fischman, Developmental Studies Hybridoma Bank, Iowa City, IA, USA). They were then visualized
 132 using anti-mouse IgG conjugate Alexa568 (Invitrogen). Nuclei were counterstained with DAPI (1
 133 mg/l). Images were acquired using an Olympus IX-51 inverted fluorescence microscope (Olympus) or
 134 Leica TCS SP8 (Leica) confocal microscope. In each repetition at least five images were taken from at
 135 least two wells for each line and the ratio between red and blue signals was analyzed using ImageJ
 136 software. The analysis of whole embryoid body staining was performed on cells cultivated in the same
 137 manner, but cells were seeded on day 5 on cover slips and on day 20 cells were not disassociated, but
 138 the whole embryoid body was fixed and stained as described above. Representative images were
 139 acquired using Leica TCS SP8 (Leica) confocal microscope.

140 The relative number of cardiomyocytes was also determined using R1_MHC-neo/pGK-hygro ES cells
 141 (HG8 cells) and their DUSP7 KO clones (MHC-neo/DUSP7 KO; analysis of frame shift mutations in
 142 both DUSP7 alleles in these cell lines by NGS shown Fig. 2A), as described previously [19]. Estimation

143 of the relative number of viable cells after antibiotic selection was performed by ATP quantification in
144 whole cell lysates. Cells were lysed in Somatic cell ATP releasing reagent for ATP determination
145 (FLSAR-1VL, Sigma-Aldrich). Each cell lysate was mixed with Cellular ATP Kit HTS (155-050,
146 BioThema) in the ratio of 1:1 and luminescence was analyzed using Microlite™ 1+ strips (Thermo
147 Scientific) and Chameleon V (Hindex).

148 *Small Interfering RNA (siRNA) Transfection*

149 Cells were transfected by commercially available siRNA DUSP6 (sc-39001) and DUSP7 (sc-61428)
150 to knock down gene expression, or by related non-silencing control (all Santa Cruz Biotechnology,
151 USA) using Lipofectamine RNAiMAX Reagents (Thermo Fisher Scientific Inc., USA) according to
152 the manufacturer's instructions. Cells were harvested 24h after transfection and the expressions of
153 selected proteins and posttranslational modification were analyzed by western blot [27].

154 *Western-blot analysis*

155 Cells were directly lysed in Laemmli buffer (100 mM Tris/HCl (pH 6.8), 20% glycerol, 1% SDS,
156 0.01% bromophenol blue, and 1% 2-mercaptoethanol). Western blotting was performed according to
157 the manufacturer's instructions with minor modifications (SDS-PAGE run at 110 V, transfer onto
158 PVDF membrane for 1 h at 110 V (BIO-RAD)). Membranes were blocked in 5% non-fat dry milk
159 solution in TBS-T for 30 min and subsequently incubated overnight at 4 °C with primary antibodies
160 listed in Table 2. Next, membranes were washed in TBS-T and incubated with HRP-conjugated
161 secondary antibodies (Sigma-Aldrich). Immunoreactive bands were detected using ECL detection
162 reagent kit (Merck-Millipore) and the FusionSL chemiluminescence documentation system (Vilber-
163 Lourmat). Results were quantified by the densitometric analysis of Western blot bands using the Fiji
164 distribution of ImageJ.

165 **Table 2.** Primary antibodies used for western-blot analysis.

Antibody	Catalog number	Company
p-ERK1/2	CS-4370S	Cell Signaling
ERK1/2	CS-4695S	Cell Signaling
PARP	9532	Cell Signaling
JNK	sc-571	Santa Cruz Biotechnology
pJNK	sc-6254	Santa Cruz Biotechnology
p-38	9212	Cell Signaling
pp-38	9211	Cell Signaling
MHC	anti-MHC, clone MF20	Developmental Studies Hybridoma Bank
βIII tubulin	Ab7751	Abcam
DUSP6	sc-377070	Santa Cruz Biotechnology
DUSP6	3058	Cell Signaling
Vinculin	V9264	Sigma
β-Actin	sc-47778	Santa Cruz Biotechnology

166

167 *Isolation of mouse hearts*

168 CD1 mice were maintained and bred under standard conditions and were used in accordance with
169 European Community Guidelines on accepted principles for the use of experimental animals. Mouse
170 hearts were isolated according to an experimental protocol that was approved by the National and

171 Institutional Ethics Committee (protocol MSMT-18110/2017-5). Individual heart samples were
172 prepared as described previously [19].

173 *Statistical Analysis*

174 Data analysis was performed by GraphPad Prism. Data are expressed as mean \pm standard deviation
175 (SD). Statistical analysis was assessed by t-test and by one- or two-way ANOVA, and by Bonferroni's
176 Multiple Comparison post hoc test. Values of $P < 0.05$ were considered to be statistically significant
177 (* $p < 0.05$).

178 **Results**

179 *Absence of DUSP7 does not affect the phenotype of ES cells*

180 In order to determine the effect of DUSP7 on ES cells, we created DUSP7 knock out (KO) cell lines
181 using the CRISPR-Cas9 system, as previously described [24], [28]. These mutated cell lines were
182 verified by NGS (Fig. 1B) and were then used for all subsequent experiments (see experimental set up
183 in Fig. 1A). All used DUSP7 KO cell lines had either the same or different mutations in individual
184 alleles, but in both cases the result was a frame shift mutation.

185 We were able to cultivate all obtained DUSP7 KO cell lines in vitro for a substantial time (40+
186 passages), during which we did not observe any morphological difference between KO and wild type
187 (WT) control (CTR) cell lines. To determine whether DUSP7 KO cell lines proliferate at a similar rate
188 we stained them on three consecutive days using crystal violet, the results indicating that there were
189 no significant differences in growth rate between WT and KO cell lines, nor between individual KO
190 lines (Fig. 2A). The same proliferation was confirmed by the EdU assay and the WST-8 assay (Fig. 2B
191 and 2C).

192 Next, we determined whether DUSP7 KO cells retain their stem cell phenotype by testing whether they
193 differ from WT cells in expressing markers which are known to change if pluripotency is compromised
194 – specifically, *Oct4*, *Nanog*, *Klf4*, *Zfp42* and *Fgf5* [29]–[33]. Cells were kept in standard culture
195 conditions for ES cells for 5-40 passages before these markers were analyzed. We did not observe any
196 statistical differences in the expressions of the given markers between any of these lines (Fig. 2D). On
197 the basis of the above, we conclude that the depletion of DUSP7 does not affect the proliferation rate
198 of ES cells nor their pluripotent phenotype.

199 *DUSP7 regulates germ layer specification in differentiating ES cells*

200 To further test their stem cell-like properties, we studied the ability of DUSP7 KO cells to differentiate.
201 All cell lines were able to form embryoid bodies (EBs) of the same shape and size in hanging drops or
202 in cell suspension culture (Fig. 3A). In 5-day-old EBs, transcripts of all three germ layers were
203 determined – namely, *Sox1* and *Pax6* as markers for ectoderm/ neuroectoderm; *T*, *Mesp1*, *Mef2c*,
204 *Gata4*, *Gata1* and *Gata2* as markers for mesoderm; and *Afp* as a marker for entoderm [34]–[39]. In
205 DUSP7 KO cells, the expressions of *T*, *Mesp1* and *Gata4* were decreased compared to WT cells, while
206 the expressions of *Sox1* and *Pax6* were increased. Excluding the expression of *Afp* in one DUSP7 KO
207 cell line, we did not observe significant differences in the levels of *Mef2c*, *Gata1*, *Gata2*, or *Afp*
208 between KO and WT cells. The increase in *Afp* was observed in only one of the DUSP7 KO cell lines,
209 indicating that it might be an artefact typical only for this individual line (Fig. 3B). These data show
210 that DUSP7 is required for the correct formation of ectoderm and mesoderm during in vitro
211 differentiation of ES cells.

212 *DUSP7 is required for cardiomyocyte formation*

213 Since we observed differences in the abilities of cells to form mesoderm and ectoderm at early stages,
214 we differentiated cells in vitro for a further 5-10 days and then studied the formation of cardiac and
215 neural cells. DUSP7 KO cells exhibited lower levels of expression of cardiomyocyte-specific
216 transcripts (*Nkx2.5*, *Myh6*, *Myh7*) and higher levels of the expression of neuro-specific markers (*Tubb3*
217 and *Mash1*) (Fig.4A). Similar difference in cardiomyogenesis and neurogenesis were observed also at
218 the protein level, where DUSP7 KO cells exhibited lower levels of cardiomyocyte-specific (MHC) and
219 higher levels of neuro-specific (β III tubulin) proteins compared to WT (Fig. 4B). To further explain the
220 observed decreases in the expressions of cardiomyocyte specific transcripts and proteins, we studied
221 the number of formed cardiomyocytes. Cells were cultivated for the first five days as hanging drops in
222 order to form single EBs. Then, each EB was individually cultivated for a total of 20 days and either
223 the whole embryoid body was stained for cardiomyocyte-specific (MHC) or neuro-specific
224 (β III tubulin) markers (Supplementary fig. 1-2) or cells were re-seeded onto a fresh plate as single cells.
225 In the latter case, after a further day of cultivation, they were stained with antibody specific for cardiac
226 myosin heavy chains (MHC) and with DAPI. The ratio between the number of nucleuses and myosin
227 positive cells, which determines the number of cardiomyocytes, was lower in DUSP7 KO cell lines
228 compared to wild type cells (Fig. 5A and 5B, Supplementary fig. 3.). In addition, we determined the
229 relative number of formed cardiomyocytes on day 20 after cardiomyocytes specific selection on HG8
230 cells and their DUSP7 KO cells (see Material and Methods). Here, we again observed that DUSP7 KO
231 cells formed a lower number of cardiomyocytes compared to WT cells (Fig. 5C). These results
232 therefore indicate that DUSP7 is required for the formation of mouse cardiomyocytes in vitro.

233 *DUSP7 depletion does not change the phosphorylation of ERK*

234 Since DUSP7 is known to dephosphorylate MAPK with a preference towards ERK1/2, we tested
235 whether there were differences between the levels of phosphorylated ERK, JNK and p38 at the basal
236 level in ES cells. However, only ERK1/2 showed any differences and these were very small and
237 deemed to be statistically insignificant (Fig. 6A). Interestingly, when using siRNA for DUSP7, we
238 also observed no change in the phosphorylation of ERK after 24h, but when using siRNA for DUSP6,
239 we saw a stronger signal for pERK1/2. (Fig 5.B). Since the phosphorylation and dephosphorylation of
240 ERK is an important process for signal transduction and very dynamic process, we tested whether there
241 would be a change in the kinetics of phosphorylation between wild type and KO cells. Cells were
242 starved for 6h in media without serum. After this time, serum was added to a final concentration of
243 30% and phosphorylation was measured by western blot method 10min, 30min, 1h and 3h after
244 stimulation. The highest phosphorylation was observed 10min after stimulation in all cell lines and
245 after 1h the level of phosphorylation had returned to its basal level. Although there were slight
246 differences between individual sets in this dynamic, neither the overall maximum level of ERK
247 phosphorylation nor the speed of dephosphorylation between wild type and KO cell lines showed
248 statistically significant differences (Fig. 6C).

249 *Level of DUSP7 increases during differentiation*

250 Since the depletion of DUSP7 did not have an effect on the basic characteristics of ES cells, (Fig. 2,
251 Fig. 6), but did have an effect on the differentiation of cells in later stages of in vitro cultivation and on
252 the differentiation of cardiomyocytes, we measured changes in the expression of *Dusp7* using RT-
253 qPCR in cells from in vitro culture (Fig. 7A) and in hearts of mice from different stages of development
254 (Fig. 7B). We found that the level of *Dusp7* increased over time during differentiation in culture as
255 well as in the hearts of mice during their ontogenesis. Therefore, since DUSP7 might have a more

256 important role in later stages of differentiation in vitro than in ES cells, we tested the level of
257 phosphorylation of ERK1/2 in 5-day-old embryoid bodies but were not able to see any significant
258 difference between the tested cell lines (Fig. 7C).

259 Discussion

260 It is generally agreed that DUSPs specifically dephosphorylate MAPKs. However, when it comes to
261 their specificity to individual proteins there are some conflicting reports about which substrates they
262 can dephosphorylate, especially when it comes to the more studied phosphatases such as DUSP1 [40]–
263 [42] or DUSP6 [43], [44], these conflicts appearing to arise because these proteins are studied in
264 different conditions or in different models. DUSP7 is generally believed to dephosphorylate ERK1/2,
265 but in some conditions was shown to interact with JNK [45]–[49]. However, there are also studies
266 which suggest the possibilities of DUSP7 dephosphorylating substrates other than members of the
267 MAPK family. It has been shown that DUSP7 can also dephosphorylate cPKC isoforms [50], thus
268 inhibiting their activity. In the case of DUSP7 depletion, the activity of cPKC is not inhibited at the
269 correct time or for the correct duration, which leads to defects in meiosis in mouse oocytes; however,
270 our data suggest that the depletion of DUSP7 does not affect the mitosis of ES cells (Fig 1B).

271 There are numerous studies which show the effects of the activation of MAPK/ERK in ES cells on
272 their stemness and differentiation [51]–[53]. The depletion of DUSP2 and its effect on ES cells was
273 also studied in association with DUSP7 by Chappell et al., who showed that DUSP7 is necessary for
274 the preservation of pluripotency [54]. However, a significant effect on pluripotency was shown only
275 when DUSP7 was overexpressed, or when DUSP7 was knocked-down together with DUSP2. In
276 contrast, our model shows that ES cells are able to adapt to long cultivation when DUSP7 is knocked-
277 out by itself (Fig. 2B).

278 During differentiation in KO cells, we observed a significant decrease in the general mesodermal
279 marker *T* as well as in *Mesp1*, which appears in the cardiogenic area of the primitive streak [55]. The
280 expression of *Gata4*, a gene necessary for normal heart tube formation [37], [56] and a regulator of
281 other genes critical for cardiomyogenesis [57], was also downregulated, unlike its cofactor *Mef2c*,
282 which is also expressed during the early development of myocardium and other muscle cells [36], [58],
283 [59]. The *Mef2c* marker was more variable between KO lines, but did not show a significant decrease
284 or increase compared to control. Although this gene is widely used as a cardiac marker, it is greatly
285 expressed also in mouse brain [60] and is crucial for normal neural development [61]; therefore, its
286 potentially lower levels due to reduced cardio myogenesis are masked by potentially higher levels in
287 developing neural progenitors. Preferential differentiation of DUSP7 KO into neuro-ectodermal
288 lineages is supported by elevated levels of *Sox1* and *Pax6*. In contrast to cardiac-mesoderm markers, the
289 levels of mesodermal markers *Gata1* and *Gata2*, which are important for the formation of
290 hematopoietic lineages, were not changed by the depletion of DUSP7. The importance of different
291 MAPK in hematopoiesis and especially in diseases such as leukemia has been studied, but it has been
292 shown that p38 α plays the key role in hematopoietic stem cell activation and, later, in their maturation
293 during hematopoiesis [62], [63]. With respect to the interaction of DUSP7 with members of the MAPK
294 family, there is least evidence that DUSP7 interacts with p38; therefore, the fact of its depletion having
295 no effect on hematopoietic markers was to be expected.

296 Several members of the DUSP family have been studied with respect to the development of heart tissue
297 or the neural system, most of them via the mechanism linked with the dephosphorylation of ERK.
298 When it comes to neural development, DUSP1, DUSP4 and DUSP6 were shown to be regulated by
299 nerve growth factor [10], [64], [65]. DUSP1 is necessary for normal axonal branching [66], similarly

300 to DUSP6, which also plays a role in normal axon development [67]. The overexpression of DUSP1
301 has a neuroprotective effect in response to ischemia [68], [69] and, together with DUSP4, they protect
302 motor axons from degradation [70]. The role of DUSP7 in neural development has not yet been
303 thoroughly studied, despite DUSP7 being expressed in whole brain of mice [71]. Our study, therefore,
304 is one of the first to show that DUSP7 can inhibit the development of neuronal lineages in an in vitro
305 model of EC cell differentiation.

306 When it comes to the development of heart, MAPK play an important role since they are highly
307 involved in FGF and BMP signaling – two very important signaling pathways playing a role in cardiac
308 mesoderm and myocardium formation. These pathways need to be almost periodically activated and
309 inhibited for normal formation of heart, which can be achieved by negative feedback mediated by
310 MAPK-induced DUSP expression [3], [72].

311 In heart, DUSPs have mostly been linked with the regulation of the ERK signaling pathway and the
312 proliferation of cardiomyocytes. In general, all studies involving the depletion of any DUSPs show
313 heart enlargement. However, in some cases, there need to be special conditions like heart exposure to
314 hypoxia for hypertrophy to be apparent [73], or hypertrophy is detectable only in adults or after
315 injury, such as in DUSP6-deficient fish [11]. Depletions of different DUSPs in mice have shown
316 changes in cardiomyocyte morphology (DUSP8 [74]), or have been linked to protection (DUSP6 [75])
317 or, in contrast, to increased susceptibility to cardiomyopathy (DUSP1, DUSP4 [76]). All of these
318 studies either operate with the measurement of hearts of adult subjects or, in the case of in vitro studies,
319 they use already differentiated or neonatal cardiomyocytes, in contrast to our study, which investigated
320 differentiation from ES cells and the effect of DUSP7 on early cardiomyocyte differentiation.

321 As mentioned before, an appropriate level of activation at the right time and for the right duration plays
322 an important role in the development of heart. For example, the activation of ERK by 12-O-
323 Tetradecanoylphorbol-13-acetate (TPA) leads to an increase in cardiomyogenesis, but only when the
324 treatment is applied in a certain time window [19]. Similarly, we see in our experiments that applying
325 TPA at the indicated time does increase the number of cardiomyocytes in our KO cell lines
326 (Supplementary fig. 4) comparably to wild types; however, already at this point, there are fewer
327 mesodermal cells on which it can have an impact, as we showed by measuring T and Mesp1 expression.
328 Furthermore, cardiomyocytes derived from KO cells have the same maturation profile as WT, as shown
329 by the ratios of *Nkx2.5*, *Myh6*, and *Myh7* [19] (Supplementary fig. 5). Therefore, it seems that DUSP7
330 plays a role in early stages of this process and does not have a big impact on later cardiomyocyte
331 development.

332 Since, as mentioned, DUSP7 is specific towards MAPK with a preference towards ERK1/2 [14], we
333 studied the levels of phosphorylation of different MAPK, but, we did not observe any significant
334 differences in our KO cell lines compared to wild type. This is in contrast to previously published
335 observations; however, some of these publications show only the slightly higher phosphorylation of
336 ERK1/2 when the expression of DUSP7 is lowered in combination with other DUSPs [54] or under
337 special conditions, such as in DUSP7 KO mice that are on a high fat diet [77]. The observation of only
338 a very small effect of DUSP7 could also be due to the fact that DUSP7 exhibited very low expression
339 in our ES cells to begin with, more than 10x lower compared, for example, to DUSP6 (Supplementary
340 fig. 6), which is reinforced by the fact that when using siRNA for DUSP6 and DUSP7 we could see
341 changes in the phosphorylation of ERK only in the former case (Figure 5B). However, unlike in many
342 studies which used siRNA or shRNA, or measured the phosphorylation levels a short time after adding
343 some inhibitors or activators, our cells were modified using CRISPR/Cas9 and were cultivated for a
344 long time, during which they might have adapted to DUSP depletion. This can be also demonstrated

345 by DUSP6, where we did not see the same effect when it was knocked out using CRISPR/Cas9 as
346 when using siRNA (Supplementary fig. 7). We also saw that the level of DUSP7 rises during
347 differentiation in vitro and in developing heart, indicating its importance in such development,
348 including the growth of myocardium. Since in our experimental design cells were being differentiated
349 through the formation of EBs, and culture conditions throughout the differentiation process did not
350 favor any individual cell type in particular, we can assume that the ones which achieved a head start
351 overgrew in the culture and “smothered” other cell types, whose differentiation might have been
352 compromised by genetic modification and which would have appeared later in the culture.

353 **Conclusion**

354 In summary, on the basis of all of our results, we can conclude that DUSP7 promotes early
355 differentiation towards neural cells and that in DUSP7 KO early cardiac mesoderm is repressed, which,
356 in prolonged cultivation, is reflected by a lower number of formed cardiomyocytes.

357 **Data Availability**

358 The data used to support the findings of this study are available from the corresponding author upon
359 request.

360 **Conflicts of interest**

361 The authors report no conflicts of interest. The authors alone are responsible for the content and writing
362 of the paper.

363 **Funding statement**

364 This research was supported by the Faculty of Science of Masaryk University (MUNI/A/1145/2017),
365 by the Czech Science Foundation (Project 18-18235S), and by a grant from the Czech Science
366 Foundation (Project 19-16861S).

367 **Figures**

368 **Figure 1.**

369 (A) Schematic representation of the different experiments conducted in this study – at what time points
370 different methods were employed and which markers were analyzed. (B) The guide RNA (gRNA)
371 design and the sequences of verified deletions in the DUSP7 KO ES cell line edited by the
372 CRISPR/Cas9 system are shown.

373

374 **Figure 2.**

375 DUSP7 KO mouse embryonic stem cells retain the basic characteristic of the cell line. (A) To assess
376 the growth curve of wild type and DUSP7 KO cell lines, 1000 cells/cm² were seeded on a fresh plate
377 on day 0 and plates were stained with crystal violet staining on days 3,4 and 5 to assess their growth
378 curve. The experiment was repeated three times and the value for individual experiments represents
379 the average value obtained from four plates. (B) To assess proliferation rate, wild type and DUSP7 KO
380 cell lines were seeded at a concentration 5000 cells/cm² and after 3 days of cultivation they were treated
381 with EdU for 1h. Graph represents mean ± SD of four independent replicates. (C) To test whether the
382 proliferation rate of DUSP7 KO cells will be different compared to wild type cells, based on cell
383 density, cells were seeded in a 96 well plate at a concentration of 1000, 500, 250, 125 and 67 cells/well.
384 Cells were cultivated for 3 days after which they were incubated with WST-8/Methoxy-PMS for 5

385 hours and relative absorbance was measured. Graph represents mean \pm SD of three independent
386 replicates. **(D)** To check whether the DUSP7 KO cell lines retained their pluripotency, known markers
387 of pluripotency *Oct4*, *Nanog*, *Zfp42*, *Ffg5* and *Klf4* were measured. Stem cells from low (around 5),
388 mid-range (around 15) and high (40+) passages were used. Graphs represent mean \pm SD of three
389 independent replicates. Differences between groups were considered to be statistically significant when
390 values of $P < 0.05$ (*).
391

392 **Figure 3.**

393 DUSP7 KO cell lines are able to differentiate into all three germ layers, but preferentially express
394 markers for ectoderm over those for mesoderm. **(A)** Measures of diameter of embryoid bodies. 400
395 cells were used to create embryoid bodies using the hanging drop method. The sizes of embryoid bodies
396 were measured on Day 5. Graph represents mean \pm SD of seven independent replicates, each of the
397 values representing the average value of at least 5 different measurements. **(B)** KO cell lines exhibit
398 lower expressions of markers typical for mesoderm or cardiacmesoderm (*T*, *Mesp1*, *Gata4*) and higher
399 expressions of markers for ectoderm (*Sox1*, *Pax6*), while markers that characterize both myogenesis
400 and neurogenesis (*Mef2c*) as well as endoderm markers (*Afp*) and markers for hematopoietic mesoderm
401 (*Gata1*, *Gata2*,) have similar expression profiles as in wild type cells. Markers were measured after 5
402 days of differentiation. Graphs represent mean \pm SD of at least three independent replicates.
403 Differences between groups were considered to be statistically significant when values of $P < 0.05$ (*).
404

405 **Figure 4.**

406 DUSP7 KOs after longer differentiation in vitro express lower levels of cardiac markers compared to
407 wild type cells. **(A)** Analysis of cardiac and neural markers on qPCR. ES cells were cultivated for 10
408 days (*Mash1*) or 14 days (*Nkx2.5*, *Myh6*, *Myh7*, *BIIIIt*) and analyzed on RT-qPCR, normalized to the
409 mean expression of *Hprt* and *Rpl* (TaqMan) or *Actb* and *Tbp* (SyberGreen). Graphs represent mean \pm
410 SD of at least four independent replicates. **(B)** Western blot analysis of cardiac (MHC) and neural
411 (BIIIItubulin) markers and their quantification (on the right) after 20 days of cell differentiation. Graphs
412 represent mean \pm SD of four independent replicates. Differences between groups were considered to
413 be statistically significant when values of $P < 0.05$ (*).
414

415 **Figure 5.**

416 DUSP7 KO cells produce a lower number of cardiomyocytes **(A)** DUSP7 KO cells form fewer
417 cardiomyocytes compared to wild type cells, as analyzed by immunocytochemistry. Cells were stained
418 after a total of 21 days of differentiation. Nucleus is shown in blue (DAPI) and cardiomyocytes in red,
419 stained by cardiac specific antibody MHC. **(B)** Quantification of number of cardiomyocytes. Graph
420 represents mean \pm SD of three independent replicates, each value representing the average value for
421 three embryoid bodies analyzed. **(C)** Number of cardiomyocytes determined in HG8 cells and their
422 DUSP7 KO. Cell selection started on day 14 and measurements were performed on day 20. Graph
423 represents mean \pm SD of four independent replicates. Differences between groups were considered to
424 be statistically significant when values of $P < 0.05$ (*).
425

426 **Figure 6.**

427 Level of phosphorylation of MAPK is the same in DUSP7 KO cells. **(A)** Levels of phosphorylation of
428 different MAPKs were measured in unstimulated wild type and DUSP7 KO ES cells. Quantitative
429 analysis of the ratios between total ERK1/2 and pERK1/2, JNK and pJNK, and p38 and pp38 are shown
430 (right). Graphs represent mean \pm SD of four independent replicates. **(B)** Downregulation of DUSP7
431 by siRNA has no effect on the phosphorylation of ERK1/2. Cells were transfected by siRNA 24h after
432 passage and lysed after a further 24h of cultivation. Transfection by scrambled siRNA (scr) was used
433 as control. **(C)** ES cells were cultivated in serum free medium for 6h (time point 0') and then the

434 phosphorylation of ERK1/2 was stimulated by adding FBS to a total 30% concentration for 10min,
435 30min, 1h and 3h before analysis. Quantitative analysis of the ratio between total ERK1/2 and
436 pERK1/2 is shown (right). Graph represents mean \pm SD of two independent replicates.

437

438 **Figure 7.**

439 Level of DUSP7 changes over time during differentiation. (A) Changes in the level of *Dusp7*
440 expression in vitro culture analyzed by qPCR. Graph represents mean \pm SD of three independent
441 replicates. (B) Level of *Dusp7* in ES cells and murine heart at different stages of its development
442 analyzed by qPCR. The level of *Dusp7* has the same pattern in both atrium (A) and ventriculus (V) at
443 each individual time-point analyzed, but it changes over time, with its lowest expression seen in ES
444 cells and its highest in adult hearts. Graph represents mean \pm SD of at least three independent replicates.
445 Differences between groups were considered to be statistically significant when values of $P < 0.05$ (*).
446 (C) Phosphorylation of ERK1/2 in embryoid bodies after 5d of in vitro cultivation.

447

448 **Supplementary Material**

449

450 **Supplementary figure 1 A.** Whole embryoid body staining of WT cells.

451 **Supplementary figure 1 B.** Whole embryoid body staining of DUSP KOa cells.

452 **Supplementary figure 1 C.** Whole embryoid body staining of DUSP KOOb cells.

453 **Supplementary figure 1 D.** Whole embryoid body staining of DUSP KOc cells.

454 **Supplementary figure 2 A.** Whole embryoid body staining of WT cells.

455 **Supplementary figure 2 B.** Whole embryoid body staining of DUSP KOa cells.

456 **Supplementary figure 2 C.** Whole embryoid body staining of DUSP KOOb cells.

457 **Supplementary figure 2 D.** Whole embryoid body staining of DUSP KOc cells.

458 **Supplementary figure 3 A.** DUSP7 KO cells form fewer cardiomyocytes compared to wild type cells,
459 as analyzed by immunocytochemistry – WT cells.

460 **Supplementary figure 3 B.** DUSP7 KO cells form fewer cardiomyocytes compared to wild type cells,
461 as analyzed by immunocytochemistry – DUSP7 KOa cells

462 **Supplementary figure 3 C.** DUSP7 KO cells form fewer cardiomyocytes compared to wild type cells,
463 as analyzed by immunocytochemistry – DUSP7 KOOb cells

464 **Supplementary figure 3 D.** DUSP7 KO cells form fewer cardiomyocytes compared to wild type cells,
465 as analyzed by immunocytochemistry – DUSP7 KOc cells

466 **Supplementary figure 4.** Addition of TPA increases the number of cardiomyocytes.

467 **Supplementary figure 5.** Cardiomyocytes derived from DUSP7 KO cells have the same maturity
468 profile as cardiomyocytes from wt cells.

469 **Supplementary figure 6.** Expression of DUSP changes during development.

470 **Supplementary figure 7.** Difference in the phosphorylation of ERK1/2 by the downregulation of
471 DUSP6.

472

473 **References**

474

475 [1] P. Huang, J. Han, and L. Hui, "MAPK signaling in inflammation-associated cancer
476 development," *Protein & Cell*, vol. 1, no. 3, Mar. 2010, doi: 10.1007/s13238-010-0019-9.

477 [2] L. Chang and M. Karin, "Mammalian MAP kinase signalling cascades," *Nature*, vol. 410, no.
478 6824, Mar. 2001, doi: 10.1038/35065000.

- 479 [3] B. A. Rose, T. Force, and Y. Wang, “Mitogen-Activated Protein Kinase Signaling in the
480 Heart: Angels Versus Demons in a Heart-Breaking Tale,” *Physiological Reviews*, vol. 90, no.
481 4, pp. 1507–1546, Oct. 2010, doi: 10.1152/physrev.00054.2009.
- 482 [4] R. Roskoski, “ERK1/2 MAP kinases: Structure, function, and regulation,” *Pharmacological
483 Research*, vol. 66, no. 2, pp. 105–143, Aug. 2012, doi: 10.1016/j.phrs.2012.04.005.
- 484 [5] C. J. Marshall, “MAP kinase kinase kinase, MAP kinase kinase and MAP kinase,” *Current
485 Opinion in Genetics & Development*, vol. 4, no. 1, pp. 82–89, Feb. 1994, doi: 10.1016/0959-
486 437X(94)90095-7.
- 487 [6] M. CAMPS, A. NICHOLS, and S. ARKINSTALL, “Dual specificity phosphatases: a gene
488 family for control of MAP kinase function,” *The FASEB Journal*, vol. 14, no. 1, pp. 6–16, Jan.
489 2000, doi: 10.1096/fasebj.14.1.6.
- 490 [7] Z. Jiapaer *et al.*, “LincU Preserves Naïve Pluripotency by Restricting ERK Activity in
491 Embryonic Stem Cells,” *Stem Cell Reports*, vol. 11, no. 2, pp. 395–409, Aug. 2018, doi:
492 10.1016/j.stemcr.2018.06.010.
- 493 [8] J. Choi *et al.*, “DUSP9 Modulates DNA Hypomethylation in Female Mouse Pluripotent Stem
494 Cells,” *Cell Stem Cell*, vol. 20, no. 5, pp. 706–719.e7, May 2017, doi:
495 10.1016/j.stem.2017.03.002.
- 496 [9] Z. Li *et al.*, “BMP4 Signaling Acts via Dual-Specificity Phosphatase 9 to Control ERK
497 Activity in Mouse Embryonic Stem Cells,” *Cell Stem Cell*, vol. 10, no. 2, pp. 171–182, Feb.
498 2012, doi: 10.1016/j.stem.2011.12.016.
- 499 [10] M. Muda *et al.*, “MKP-3, a Novel Cytosolic Protein-tyrosine Phosphatase That Exemplifies a
500 New Class of Mitogen-activated Protein Kinase Phosphatase,” *Journal of Biological
501 Chemistry*, vol. 271, no. 8, pp. 4319–4326, Feb. 1996, doi: 10.1074/jbc.271.8.4319.
- 502 [11] M. A. Missinato *et al.*, “Dusp6 attenuates Ras/MAPK signaling to limit zebrafish heart
503 regeneration,” *Development*, Jan. 2018, doi: 10.1242/dev.157206.
- 504 [12] R. Lang and F. Raffi, “Dual-Specificity Phosphatases in Immunity and Infection: An Update,”
505 *International Journal of Molecular Sciences*, vol. 20, no. 11, p. 2710, Jun. 2019, doi:
506 10.3390/ijms20112710.
- 507 [13] P. P. Ruvolo, “Role of protein phosphatases in the cancer microenvironment,” *Biochimica et
508 Biophysica Acta (BBA) - Molecular Cell Research*, vol. 1866, no. 1, pp. 144–152, Jan. 2019,
509 doi: 10.1016/j.bbamcr.2018.07.006.
- 510 [14] M. Camps *et al.*, “Catalytic Activation of the Phosphatase MKP-3 by ERK2 Mitogen-
511 Activated Protein Kinase,” *Science*, vol. 280, no. 5367, pp. 1262–1265, May 1998, doi:
512 10.1126/science.280.5367.1262.
- 513 [15] O. Levy-Nissenbaum, O. Sagi-Assif, P. Raanani, A. Avigdor, I. Ben-Bassat, and I. P. Witz,
514 “Overexpression of the dual-specificity MAPK phosphatase PYST2 in acute leukaemia,”
515 *Cancer Letters*, vol. 199, no. 2, Sep. 2003, doi: 10.1016/S0304-3835(03)00352-5.

- 516 [16] W. Peng, J. Huang, L. Yang, A. Gong, and Y.-Y. Mo, “Linc-RoR promotes MAPK/ERK
517 signaling and confers estrogen-independent growth of breast cancer,” *Molecular Cancer*, vol.
518 16, no. 1, Dec. 2017, doi: 10.1186/s12943-017-0727-3.
- 519 [17] T. Luan *et al.*, “Long non-coding RNA MIAT promotes breast cancer progression and
520 functions as ceRNA to regulate DUSP7 expression by sponging miR-155-5p,” *Oncotarget*,
521 vol. 8, no. 44, Sep. 2017, doi: 10.18632/oncotarget.19190.
- 522 [18] G. T. Lountos, B. P. Austin, J. E. Tropea, and D. S. Waugh, “Structure of human dual-
523 specificity phosphatase 7, a potential cancer drug target,” *Acta Crystallographica Section F*
524 *Structural Biology Communications*, vol. 71, no. 6, pp. 650–656, Jun. 2015, doi:
525 10.1107/S2053230X1500504X.
- 526 [19] K. A. Radaszkiewicz *et al.*, “12-O-Tetradecanoylphorbol-13-acetate increases
527 cardiomyogenesis through PKC/ERK signaling,” *Scientific Reports*, vol. 10, no. 1, p. 15922,
528 Dec. 2020, doi: 10.1038/s41598-020-73074-4.
- 529 [20] K. A. Radaszkiewicz *et al.*, “The acceleration of cardiomyogenesis in embryonic stem cells in
530 vitro by serum depletion does not increase the number of developed cardiomyocytes,” *PLOS*
531 *ONE*, vol. 12, no. 3, p. e0173140, Mar. 2017, doi: 10.1371/journal.pone.0173140.
- 532 [21] A. Andersson-Rolf, A. Merenda, R. C. Mustata, T. Li, S. Dietmann, and B.-K. Koo,
533 “Simultaneous paralogue knockout using a CRISPR-concatemer in mouse small intestinal
534 organoids,” *Developmental Biology*, vol. 420, no. 2, pp. 271–277, Dec. 2016, doi:
535 10.1016/j.ydbio.2016.10.016.
- 536 [22] M. Jinek, K. Chylinski, I. Fonfara, M. Hauer, J. A. Doudna, and E. Charpentier, “A
537 Programmable Dual-RNA–Guided DNA Endonuclease in Adaptive Bacterial Immunity,”
538 *Science*, vol. 337, no. 6096, pp. 816–821, Aug. 2012, doi: 10.1126/science.1225829.
- 539 [23] K. Labun, T. G. Montague, M. Krause, Y. N. Torres Cleuren, H. Tjeldnes, and E. Valen,
540 “CHOPCHOP v3: expanding the CRISPR web toolbox beyond genome editing,” *Nucleic*
541 *Acids Research*, vol. 47, no. W1, pp. W171–W174, Jul. 2019, doi: 10.1093/nar/gkz365.
- 542 [24] F. A. Ran, P. D. Hsu, J. Wright, V. Agarwala, D. A. Scott, and F. Zhang, “Genome
543 engineering using the CRISPR-Cas9 system,” *Nature Protocols*, vol. 8, no. 11, pp. 2281–2308,
544 Nov. 2013, doi: 10.1038/nprot.2013.143.
- 545 [25] J. Malcikova *et al.*, “Detailed analysis of therapy-driven clonal evolution of TP53 mutations in
546 chronic lymphocytic leukemia,” *Leukemia*, vol. 29, no. 4, pp. 877–885, Apr. 2015, doi:
547 10.1038/leu.2014.297.
- 548 [26] J. Navrátilová *et al.*, “Selective elimination of neuroblastoma cells by synergistic effect of Akt
549 kinase inhibitor and tetrathiomolybdate,” *Journal of Cellular and Molecular Medicine*, vol.
550 21, no. 9, pp. 1859–1869, Sep. 2017, doi: 10.1111/jcmm.13106.
- 551 [27] J. Kučera *et al.*, “Hypoxia Downregulates MAPK/ERK but Not STAT3 Signaling in ROS-
552 Dependent and HIF-1-Independent Manners in Mouse Embryonic Stem Cells,” *Oxidative*
553 *Medicine and Cellular Longevity*, vol. 2017, pp. 1–16, 2017, doi: 10.1155/2017/4386947.

- 554 [28] V. T. Chu *et al.*, “Increasing the efficiency of homology-directed repair for CRISPR-Cas9-
555 induced precise gene editing in mammalian cells,” *Nature Biotechnology*, vol. 33, no. 5, pp.
556 543–548, May 2015, doi: 10.1038/nbt.3198.
- 557 [29] G. J. PAN, Z. Y. CHANG, H. R. SCHÖLER, and D. PEI, “Stem cell pluripotency and
558 transcription factor Oct4,” *Cell Research*, vol. 12, no. 5–6, pp. 321–329, Dec. 2002, doi:
559 10.1038/sj.cr.7290134.
- 560 [30] G. Pan and J. A. Thomson, “Nanog and transcriptional networks in embryonic stem cell
561 pluripotency,” *Cell Research*, vol. 17, no. 1, pp. 42–49, Jan. 2007, doi: 10.1038/sj.cr.7310125.
- 562 [31] K. Takahashi and S. Yamanaka, “Induction of Pluripotent Stem Cells from Mouse Embryonic
563 and Adult Fibroblast Cultures by Defined Factors,” *Cell*, vol. 126, no. 4, pp. 663–676, Aug.
564 2006, doi: 10.1016/j.cell.2006.07.024.
- 565 [32] G. Martello, P. Bertone, and A. Smith, “Identification of the missing pluripotency mediator
566 downstream of leukaemia inhibitory factor,” *The EMBO Journal*, vol. 32, no. 19, pp. 2561–
567 2574, Aug. 2013, doi: 10.1038/emboj.2013.177.
- 568 [33] J. Rathjen, J. A. Lake, M. D. Bettess, J. M. Washington, G. Chapman, and P. D. Rathjen,
569 “Formation of a primitive ectoderm like cell population, EPL cells, from ES cells in response
570 to biologically derived factors.,” *Journal of cell science*, vol. 112 (Pt 5), pp. 601–12, Mar.
571 1999.
- 572 [34] S. Kitajima, A. Takagi, T. Inoue, and Y. Saga, “MesP1 and MesP2 are essential for the
573 development of cardiac mesoderm.,” *Development (Cambridge, England)*, vol. 127, no. 15,
574 pp. 3215–26, Aug. 2000.
- 575 [35] A. Bondue *et al.*, “Mesp1 Acts as a Master Regulator of Multipotent Cardiovascular
576 Progenitor Specification,” *Cell Stem Cell*, vol. 3, no. 1, pp. 69–84, Jul. 2008, doi:
577 10.1016/j.stem.2008.06.009.
- 578 [36] Q. Lin, J. Schwarz, C. Bucana, and E. N. Olson, “Control of Mouse Cardiac Morphogenesis
579 and Myogenesis by Transcription Factor MEF2C,” *Science*, vol. 276, no. 5317, pp. 1404–
580 1407, May 1997, doi: 10.1126/science.276.5317.1404.
- 581 [37] J. D. Molkenin, Q. Lin, S. A. Duncan, and E. N. Olson, “Requirement of the transcription
582 factor GATA4 for heart tube formation and ventral morphogenesis.,” *Genes & Development*,
583 vol. 11, no. 8, pp. 1061–1072, Apr. 1997, doi: 10.1101/gad.11.8.1061.
- 584 [38] M. Pekkanen-Mattila *et al.*, “Spatial and temporal expression pattern of germ layer markers
585 during human embryonic stem cell differentiation in embryoid bodies,” *Histochemistry and*
586 *Cell Biology*, vol. 133, no. 5, pp. 595–606, May 2010, doi: 10.1007/s00418-010-0689-7.
- 587 [39] M. H. Lentjes, H. E. Niessen, Y. Akiyama, A. P. de Bruïne, V. Melotte, and M. van Engeland,
588 “The emerging role of GATA transcription factors in development and disease,” *Expert*
589 *Reviews in Molecular Medicine*, vol. 18, p. e3, Mar. 2016, doi: 10.1017/erm.2016.2.
- 590 [40] D. N. Slack, O.-M. Seternes, M. Gabrielsen, and S. M. Keyse, “Distinct Binding Determinants
591 for ERK2/p38 α and JNK MAP Kinases Mediate Catalytic Activation and Substrate Selectivity

- 592 of MAP Kinase Phosphatase-1,” *Journal of Biological Chemistry*, vol. 276, no. 19, pp. 16491–
593 16500, May 2001, doi: 10.1074/jbc.M010966200.
- 594 [41] J.-M. Brondello, J. Pouyssegur, and F. R. McKenzie, “Reduced MAP Kinase Phosphatase-1
595 Degradation After p42/p44^{MAPK}-Dependent Phosphorylation,” *Science*, vol. 286, no. 5449,
596 Dec. 1999, doi: 10.1126/science.286.5449.2514.
- 597 [42] S. Bandyopadhyay *et al.*, “A human MAP kinase interactome,” *Nature Methods*, vol. 7, no.
598 10, pp. 801–805, Oct. 2010, doi: 10.1038/nmeth.1506.
- 599 [43] S. Kamakura, T. Moriguchi, and E. Nishida, “Activation of the Protein Kinase ERK5/BMK1
600 by Receptor Tyrosine Kinases,” *Journal of Biological Chemistry*, vol. 274, no. 37, pp. 26563–
601 26571, Sep. 1999, doi: 10.1074/jbc.274.37.26563.
- 602 [44] R. S. Arkell, R. J. Dickinson, M. Squires, S. Hayat, S. M. Keyse, and S. J. Cook,
603 “DUSP6/MKP-3 inactivates ERK1/2 but fails to bind and inactivate ERK5,” *Cellular*
604 *Signalling*, vol. 20, no. 5, pp. 836–843, May 2008, doi: 10.1016/j.cellsig.2007.12.014.
- 605 [45] O. Bermudez, G. Pagès, and C. Gimond, “The dual-specificity MAP kinase phosphatases:
606 critical roles in development and cancer,” *American Journal of Physiology-Cell Physiology*,
607 vol. 299, no. 2, pp. C189–C202, Aug. 2010, doi: 10.1152/ajpcell.00347.2009.
- 608 [46] C. J. Caunt and S. M. Keyse, “Dual-specificity MAP kinase phosphatases (MKPs),” *The FEBS*
609 *Journal*, vol. 280, no. 2, pp. 489–504, Jan. 2013, doi: 10.1111/j.1742-4658.2012.08716.x.
- 610 [47] C. J. Caunt, S. P. Armstrong, C. A. Rivers, M. R. Norman, and C. A. McArdle,
611 “Spatiotemporal Regulation of ERK2 by Dual Specificity Phosphatases,” *Journal of*
612 *Biological Chemistry*, vol. 283, no. 39, pp. 26612–26623, Sep. 2008, doi:
613 10.1074/jbc.M801500200.
- 614 [48] S. Dowd, A. A. Sneddon, and S. M. Keyse, “Isolation of the human genes encoding the pyst1
615 and Pyst2 phosphatases: characterisation of Pyst2 as a cytosolic dual-specificity MAP kinase
616 phosphatase and its catalytic activation by both MAP and SAP kinases,” *Journal of cell*
617 *science*, vol. 111 (Pt 22), Nov. 1998.
- 618 [49] L.-N. Orlev, B. Ehud, B.-G. Tamar, S.-A. Orit, K. Yoel, and I. P. Witz, “Does the dual-
619 specificity MAPK phosphatase Pyst2-L lead a monogamous relationship with the Erk2
620 protein?,” *Immunology Letters*, vol. 92, no. 1–2, Mar. 2004, doi: 10.1016/j.imlet.2003.11.024.
- 621 [50] T. Tischer and M. Schuh, “The Phosphatase Dusp7 Drives Meiotic Resumption and
622 Chromosome Alignment in Mouse Oocytes,” *Cell Reports*, vol. 17, no. 5, Oct. 2016, doi:
623 10.1016/j.celrep.2016.10.007.
- 624 [51] T. Matsuda, “STAT3 activation is sufficient to maintain an undifferentiated state of mouse
625 embryonic stem cells,” *The EMBO Journal*, vol. 18, no. 15, pp. 4261–4269, Aug. 1999, doi:
626 10.1093/emboj/18.15.4261.
- 627 [52] T. Burdon, C. Tracey, I. Chambers, J. Nichols, and A. Smith, “Suppression of SHP-2 and
628 ERK Signalling Promotes Self-Renewal of Mouse Embryonic Stem Cells,” *Developmental*
629 *Biology*, vol. 210, no. 1, pp. 30–43, Jun. 1999, doi: 10.1006/dbio.1999.9265.

- 630 [53] H. Niwa, K. Ogawa, D. Shimosato, and K. Adachi, “A parallel circuit of LIF signalling
631 pathways maintains pluripotency of mouse ES cells.,” *Nature*, vol. 460, no. 7251, pp. 118–22,
632 Jul. 2009, doi: 10.1038/nature08113.
- 633 [54] J. Chappell, Y. Sun, A. Singh, and S. Dalton, “MYC/MAX control ERK signaling and
634 pluripotency by regulation of dual-specificity phosphatases 2 and 7,” *Genes & Development*,
635 vol. 27, no. 7, Apr. 2013, doi: 10.1101/gad.211300.112.
- 636 [55] Y. Liu *et al.*, “Mesp1 Marked Cardiac Progenitor Cells Repair Infarcted Mouse Hearts,”
637 *Scientific Reports*, vol. 6, no. 1, p. 31457, Aug. 2016, doi: 10.1038/srep31457.
- 638 [56] C. T. Kuo *et al.*, “GATA4 transcription factor is required for ventral morphogenesis and heart
639 tube formation.,” *Genes & Development*, vol. 11, no. 8, pp. 1048–1060, Apr. 1997, doi:
640 10.1101/gad.11.8.1048.
- 641 [57] A. E. Yilbas *et al.*, “Activation of GATA4 gene expression at the early stage of cardiac
642 specification,” *Frontiers in Chemistry*, vol. 2, Mar. 2014, doi: 10.3389/fchem.2014.00012.
- 643 [58] J. W. Vincentz, R. M. Barnes, B. A. Firulli, S. J. Conway, and A. B. Firulli, “Cooperative
644 interaction of *Nkx2.5* and *Mef2c* transcription factors during heart development,”
645 *Developmental Dynamics*, vol. 237, no. 12, pp. 3809–3819, Dec. 2008, doi:
646 10.1002/dvdy.21803.
- 647 [59] D. G. Edmondson, G. E. Lyons, J. F. Martin, and E. N. Olson, “Mef2 gene expression marks
648 the cardiac and skeletal muscle lineages during mouse embryogenesis.,” *Development*
649 (*Cambridge, England*), vol. 120, no. 5, pp. 1251–63, May 1994.
- 650 [60] X. Lin, S. Shah, and R. F. Balleit, “The expression of MEF2 genes is implicated in CNS
651 neuronal differentiation,” *Molecular Brain Research*, vol. 42, no. 2, pp. 307–316, Dec. 1996,
652 doi: 10.1016/S0169-328X(96)00135-0.
- 653 [61] H. Li *et al.*, “Transcription factor MEF2C influences neural stem/progenitor cell
654 differentiation and maturation in vivo,” *Proceedings of the National Academy of Sciences*, vol.
655 105, no. 27, pp. 9397–9402, Jul. 2008, doi: 10.1073/pnas.0802876105.
- 656 [62] C. R. Geest and P. J. Coffey, “MAPK signaling pathways in the regulation of hematopoiesis,”
657 *Journal of Leukocyte Biology*, vol. 86, no. 2, pp. 237–250, Aug. 2009, doi:
658 10.1189/jlb.0209097.
- 659 [63] K. Štefková *et al.*, “MAPK p38alpha Kinase Influences Haematopoiesis in Embryonic Stem
660 Cells,” *Stem Cells International*, vol. 2019, pp. 1–16, Jun. 2019, doi: 10.1155/2019/5128135.
- 661 [64] A. Misra-Press, C. S. Rim, H. Yao, M. S. Roberson, and P. J. S. Stork, “A Novel Mitogen-
662 activated Protein Kinase Phosphatase. STRUCTURE, EXPRESSION, AND REGULATION,”
663 *Journal of Biological Chemistry*, vol. 270, no. 24, pp. 14587–14596, Jun. 1995, doi:
664 10.1074/jbc.270.24.14587.
- 665 [65] Pérez-Sen *et al.*, “Dual-Specificity Phosphatase Regulation in Neurons and Glial Cells,”
666 *International Journal of Molecular Sciences*, vol. 20, no. 8, p. 1999, Apr. 2019, doi:
667 10.3390/ijms20081999.

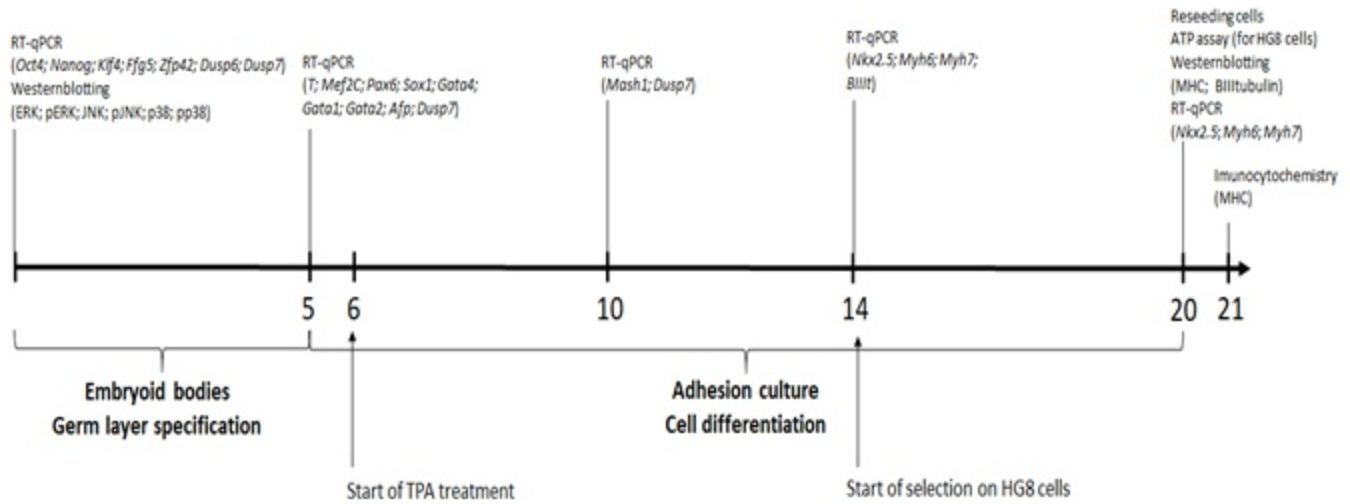
- 668 [66] F. Jeanneteau, K. Deinhardt, G. Miyoshi, A. M. Bennett, and M. v Chao, “The MAP kinase
669 phosphatase MKP-1 regulates BDNF-induced axon branching,” *Nature Neuroscience*, vol. 13,
670 no. 11, Nov. 2010, doi: 10.1038/nn.2655.
- 671 [67] M. J. Finelli, K. J. Murphy, L. Chen, and H. Zou, “Differential Phosphorylation of Smad1
672 Integrates BMP and Neurotrophin Pathways through Erk/Dusp in Axon Development,” *Cell*
673 *Reports*, vol. 3, no. 5, pp. 1592–1606, May 2013, doi: 10.1016/j.celrep.2013.04.011.
- 674 [68] L. M. Collins *et al.*, “Mitogen-Activated Protein Kinase Phosphatase (MKP)-1 as a
675 Neuroprotective Agent: Promotion of the Morphological Development of Midbrain
676 Dopaminergic Neurons,” *NeuroMolecular Medicine*, vol. 15, no. 2, pp. 435–446, Jun. 2013,
677 doi: 10.1007/s12017-013-8230-5.
- 678 [69] S. Koga, S. Kojima, T. Kishimoto, S. Kuwabara, and A. Yamaguchi, “Over-expression of map
679 kinase phosphatase-1 (MKP-1) suppresses neuronal death through regulating JNK signaling in
680 hypoxia/re-oxygenation,” *Brain Research*, vol. 1436, pp. 137–146, Feb. 2012, doi:
681 10.1016/j.brainres.2011.12.004.
- 682 [70] A. Chandrasekhar, P. Komirishetty, A. Areti, A. Krishnan, and D. W. Zochodne, “Dual
683 Specificity Phosphatases Support Axon Plasticity and Viability,” *Molecular Neurobiology*,
684 vol. 58, no. 1, pp. 391–407, Jan. 2021, doi: 10.1007/s12035-020-02119-6.
- 685 [71] B. P. Sokolov, O. O. Poleskaya, and G. R. Uhl, “Mouse brain gene expression changes after
686 acute and chronic amphetamine,” *Journal of Neurochemistry*, vol. 84, no. 2, pp. 244–252, Jan.
687 2003, doi: 10.1046/j.1471-4159.2003.01523.x.
- 688 [72] S. L. Dunwoodie, “Combinatorial signaling in the heart orchestrates cardiac induction, lineage
689 specification and chamber formation,” *Seminars in Cell & Developmental Biology*, vol. 18, no.
690 1, pp. 54–66, Feb. 2007, doi: 10.1016/j.semcdb.2006.12.003.
- 691 [73] Y. Jin *et al.*, “Mice deficient in *Mkp-1* develop more severe pulmonary hypertension and
692 greater lung protein levels of arginase in response to chronic hypoxia,” *American Journal of*
693 *Physiology-Heart and Circulatory Physiology*, vol. 298, no. 5, pp. H1518–H1528, May 2010,
694 doi: 10.1152/ajpheart.00813.2009.
- 695 [74] R. Liu, J. H. van Berlo, A. J. York, R. J. Vagnozzi, M. Maillet, and J. D. Molkentin, “DUSP8
696 Regulates Cardiac Ventricular Remodeling by Altering ERK1/2 Signaling,” *Circulation*
697 *Research*, vol. 119, no. 2, pp. 249–260, Jul. 2016, doi: 10.1161/CIRCRESAHA.115.308238.
- 698 [75] M. Maillet, N. H. Purcell, M. A. Sargent, A. J. York, O. F. Bueno, and J. D. Molkentin,
699 “DUSP6 (MKP3) Null Mice Show Enhanced ERK1/2 Phosphorylation at Baseline and
700 Increased Myocyte Proliferation in the Heart Affecting Disease Susceptibility,” *Journal of*
701 *Biological Chemistry*, vol. 283, no. 45, pp. 31246–31255, Nov. 2008, doi:
702 10.1074/jbc.M806085200.
- 703 [76] M. Auger-Messier *et al.*, “Unrestrained p38 MAPK Activation in *Dusp1/4* Double-Null Mice
704 Induces Cardiomyopathy,” *Circulation Research*, vol. 112, no. 1, pp. 48–56, Jan. 2013, doi:
705 10.1161/CIRCRESAHA.112.272963.

706 [77] L. Wu, Y. Liu, Y. Zhao, M. Li, and L. Guo, “Targeting DUSP7 signaling alleviates hepatic
707 steatosis, inflammation and oxidative stress in high fat diet (HFD)-fed mice via suppression of
708 TAK1,” *Free Radical Biology and Medicine*, vol. 153, Jun. 2020, doi:
709 10.1016/j.freeradbiomed.2020.04.009.

710

Figure 1.

(A)

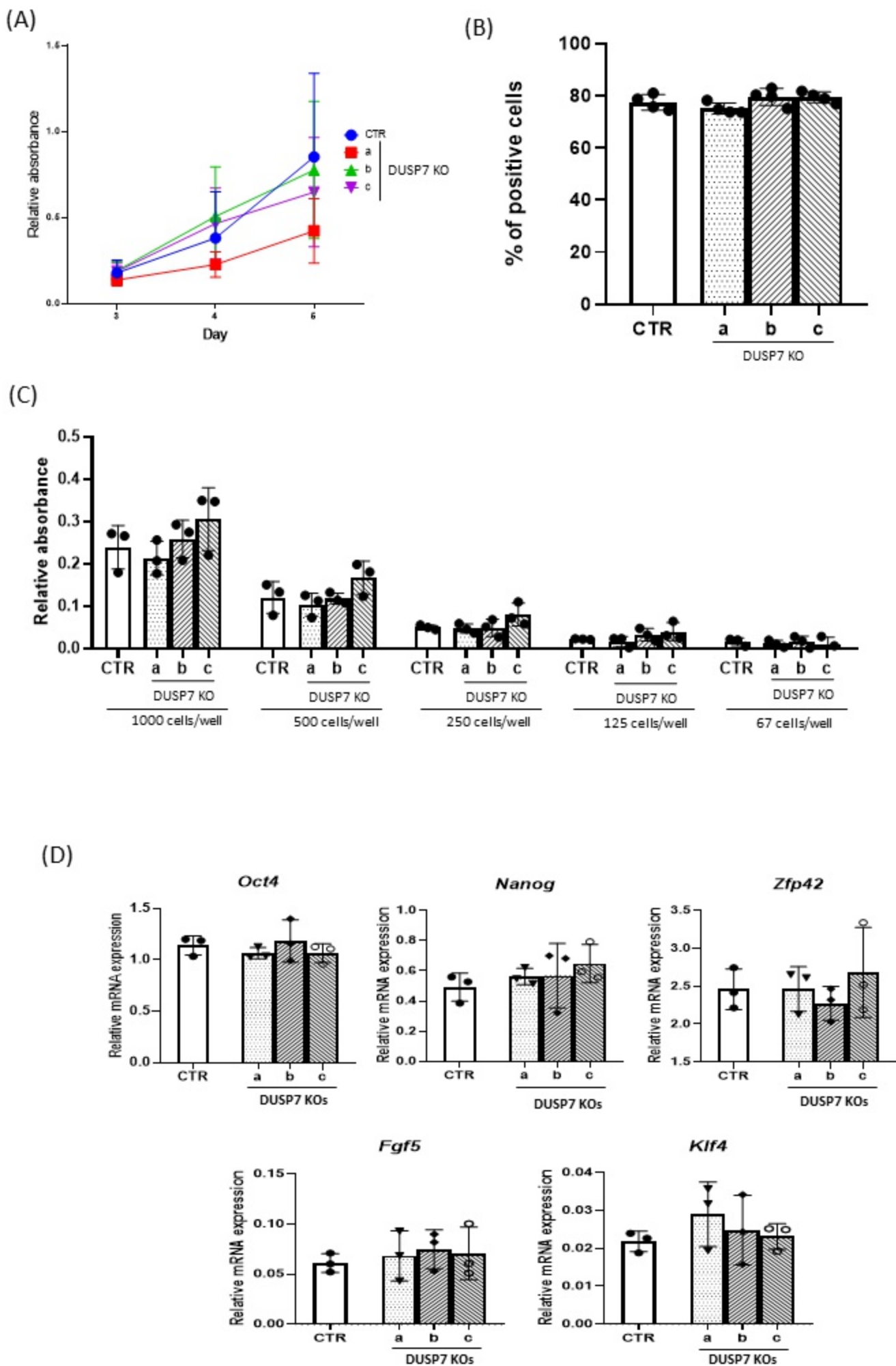


(B)

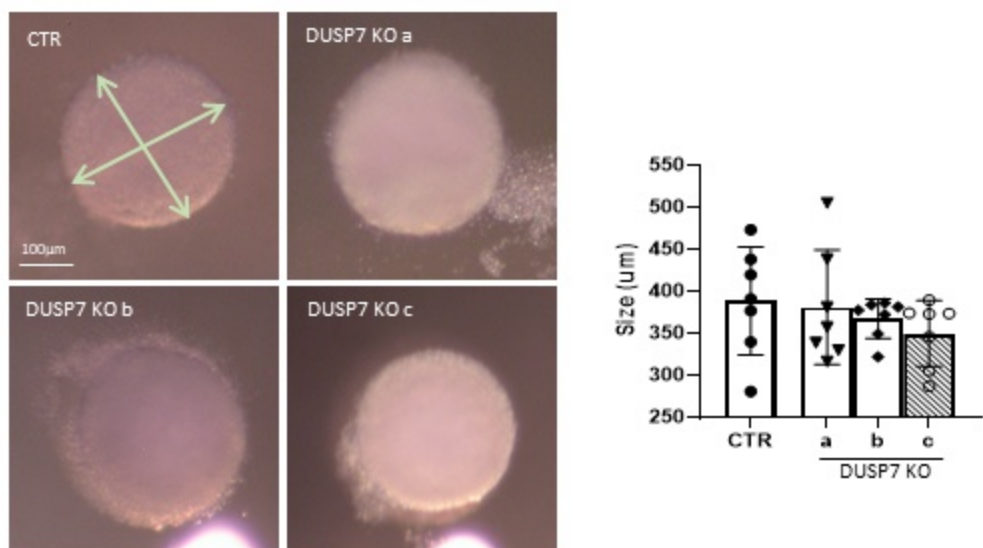
<i>Dusp7</i> gRNA	CGAGCATTGTGAGACTAACGTGG	
WT DUSP7	TACTCCGAGCATTGTGAGACTAACGTGGACAGCTCGTCCT	
KO a	TACTCCGAGCATTGTGA-----GACAGCTCGTCCT	TACTCCGAGCATTGTGAGACT-ACGTGGACAGCTCGTCCT
KO b	TACTCCGAGCATTGTGA-----GACAGCTCGTCCT	TACTCCGAGCATTGTGA-----GACAGCTCGTCCT
KO c	TACTCCGAGCATTGTGAGACTA--GTGGACAGCTCGTCCT	TACTCCGAGCATTGTGAGACTA--GTGGACAGCTCGTCCT
Hg8 a	TACTCCGAGCATTGTGAGAC-AACGTGGACAGCTCGTCCT	TACTCCGAGCATTGTGAGACTA---GACAGCTCGTCCT
Hg8 b	TACTCCGAGCATTGTGAGACTAA-----TCGTCCT	TACTCCGAGCATTGTGAGACTAA-----TCGTCCT
Hg8 c	TACTCCGAGC-----AACGTGGACAGCTCGTCCT	TACTCCGAGCATTGTGAGAC-----TCCT

Figure 2.

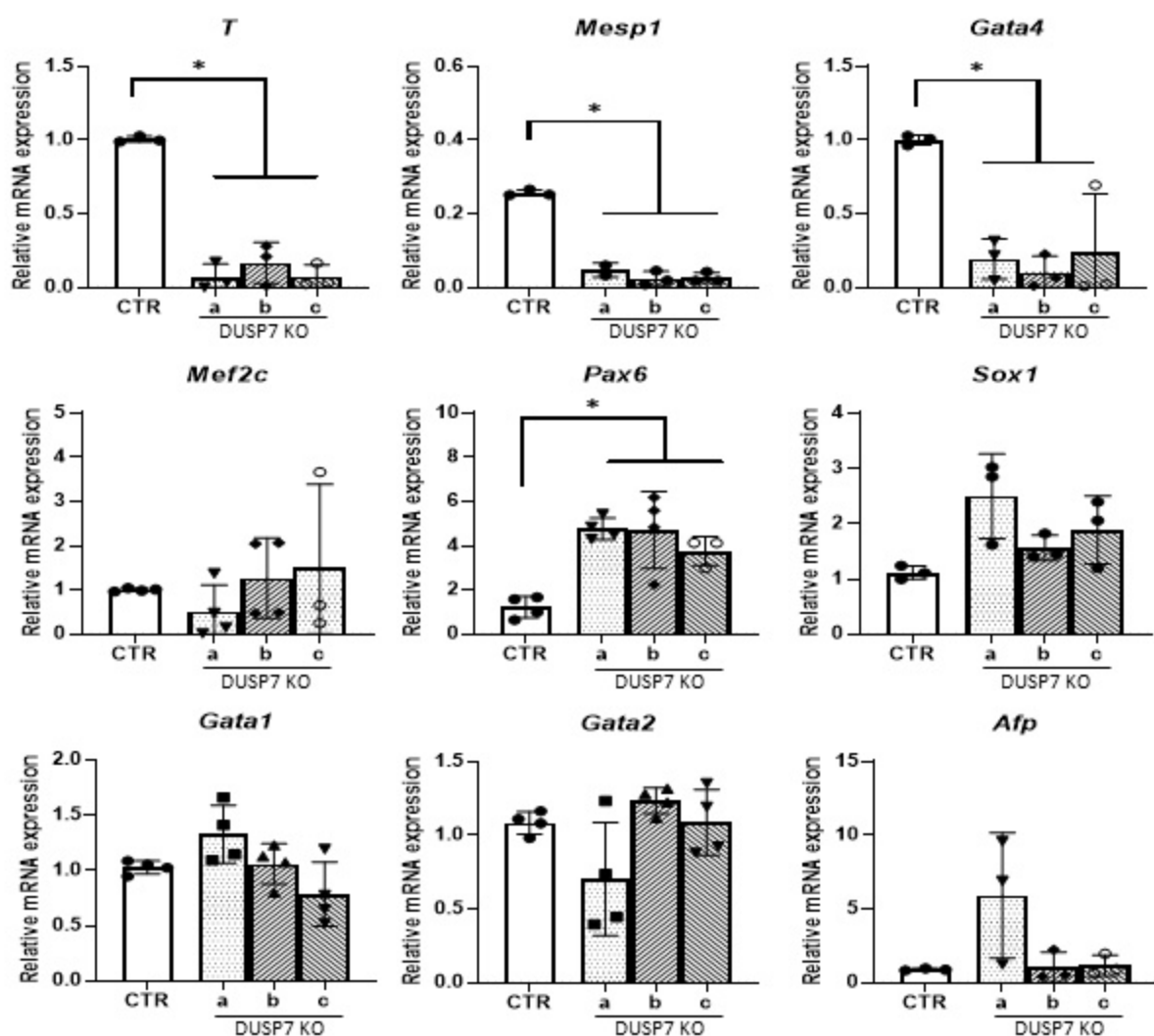
(which was not certified by peer review) is the author/funder, who has granted bioRxiv a license to display the preprint in perpetuity. It is made available under aCC-BY-ND 4.0 International license.



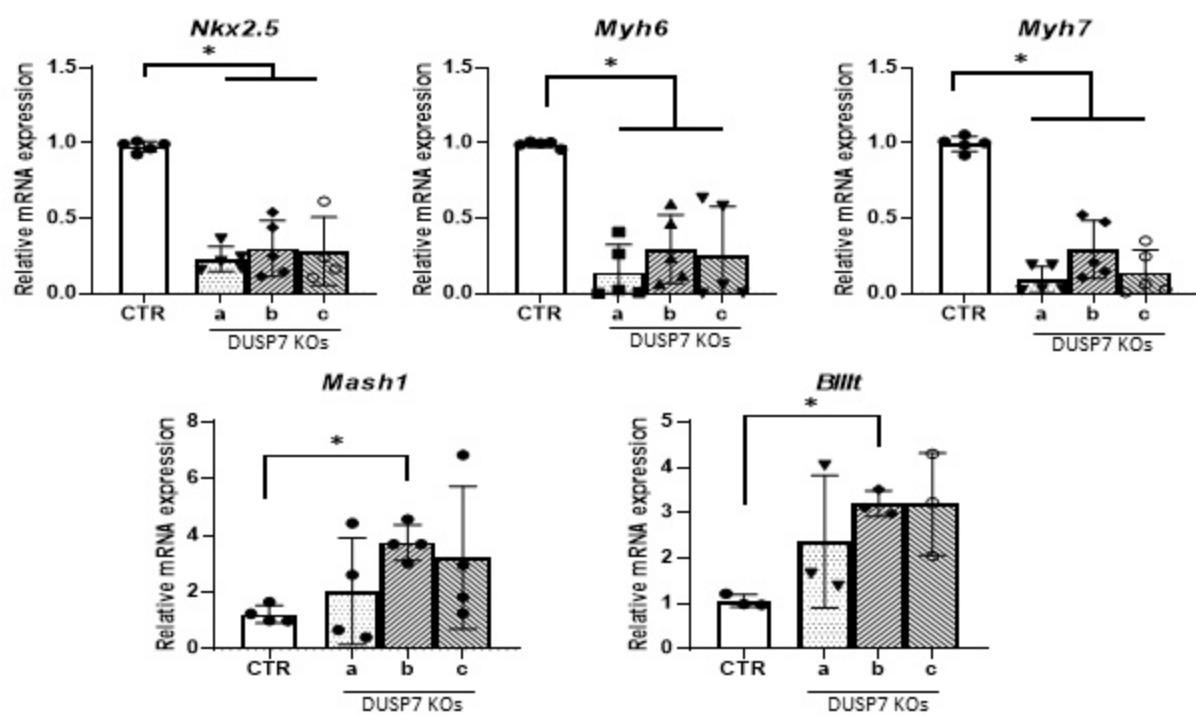
(A)



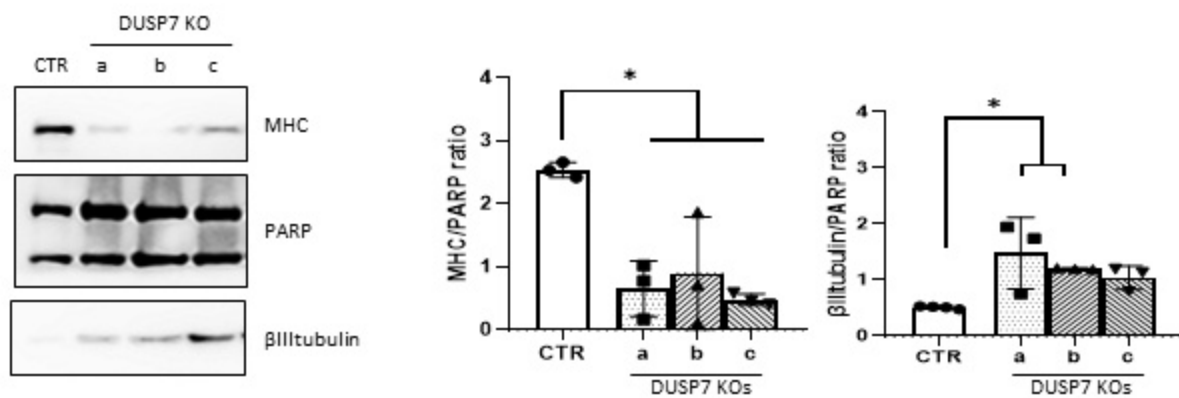
(B)



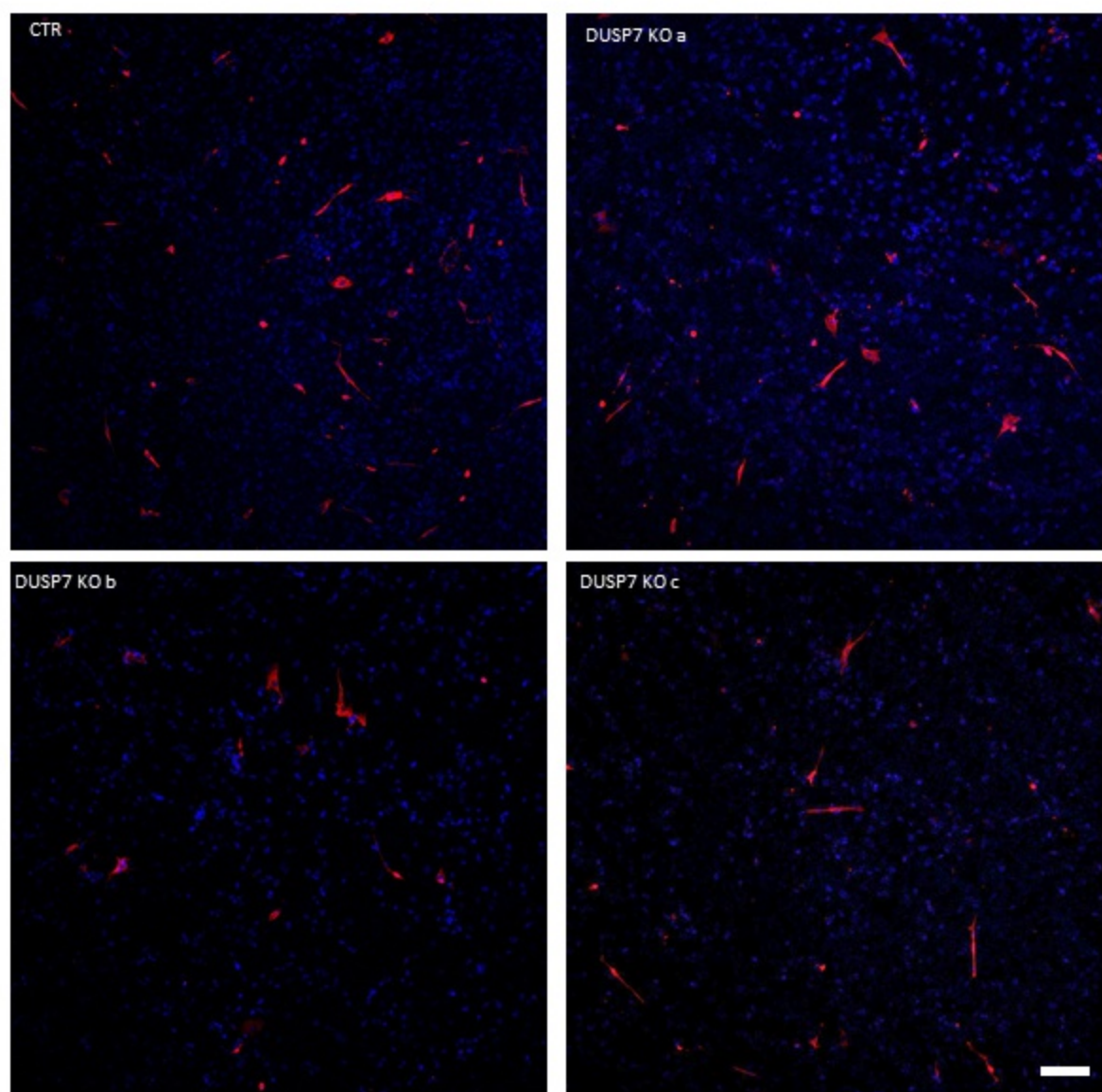
(A)



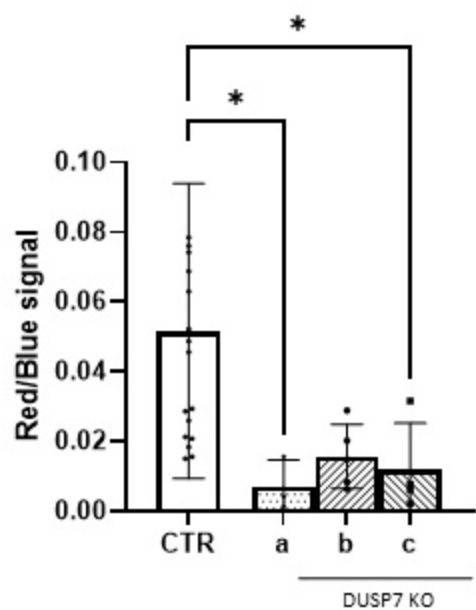
(B)



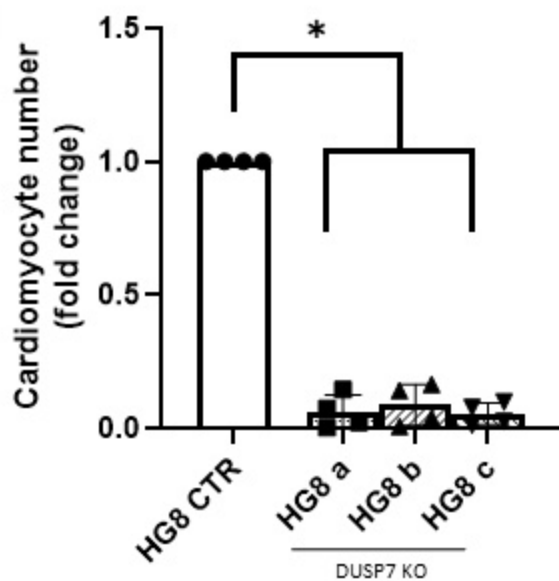
(A)

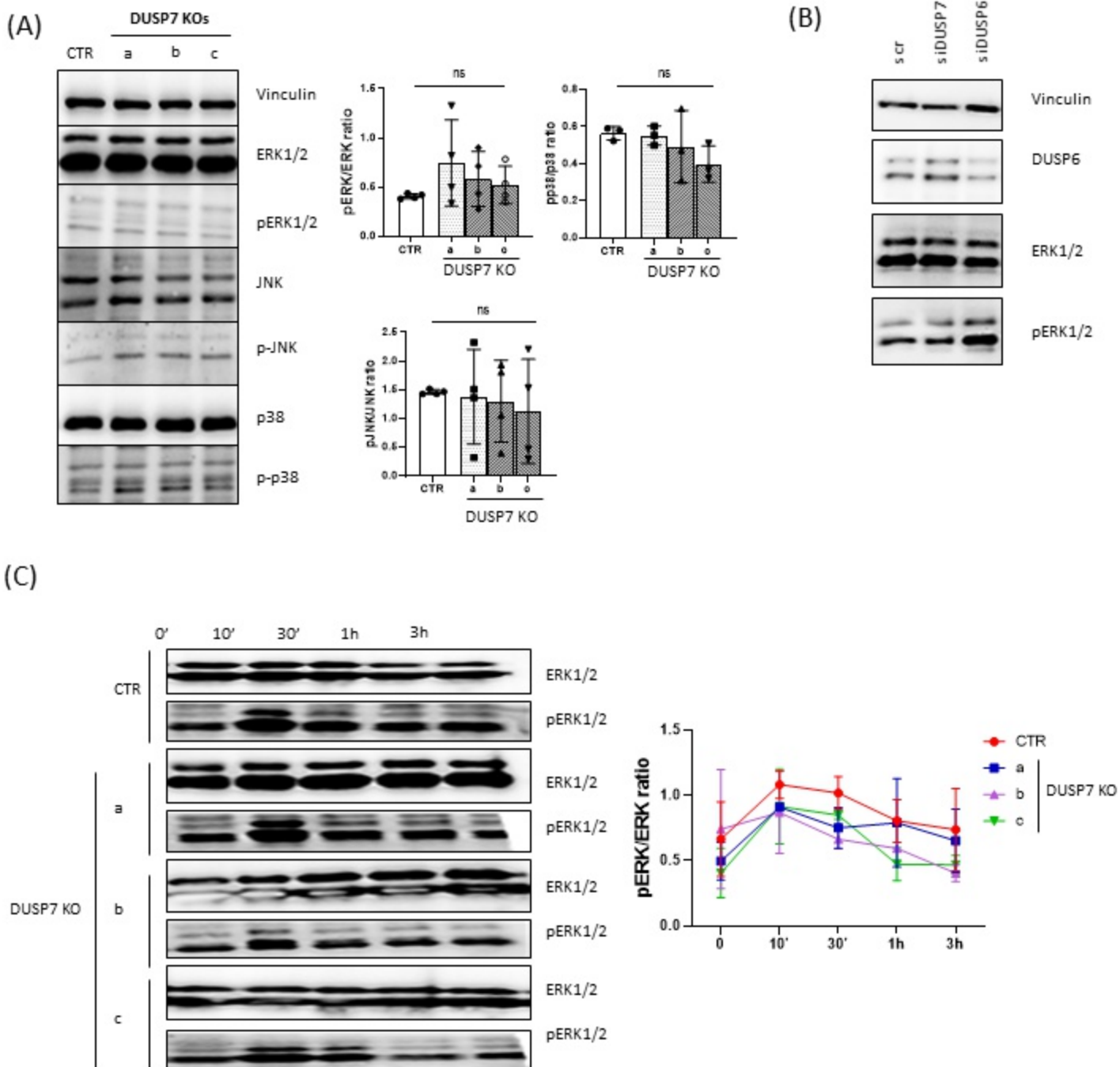


(B)

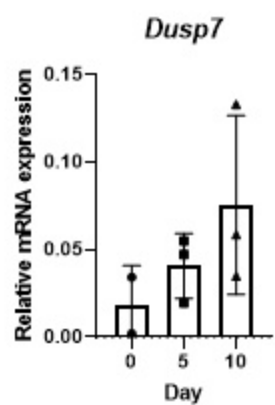


(C)

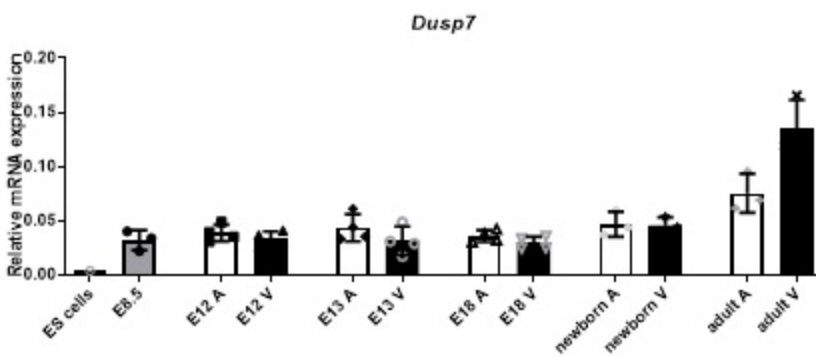




(A)



(B)



(C)

